



A Flexible, Highly Sensitive Porous PDMS Tactile Sensor Based on the Physical Foaming Method

Zichen Song¹ · Le Zhao¹ · Chunlei Chang¹ · Yan Zhou¹ · Wenxing An¹ · Shihui Yu²

Received: 29 May 2022 / Accepted: 12 September 2022 / Published online: 14 October 2022
© The Minerals, Metals & Materials Society 2022

Abstract

Flexible pressure sensors have received wide attention due to their potential applications in wearable electronics and electronic skins. It is still a challenge to manufacture high-sensitivity flexible pressure sensors in a low-cost and efficient way. In this study, a low-cost and simple method for preparing a flexible pressure sensor with porous structure based on physical foaming is proposed. The sensitivity of the flexible pressure sensor is 0.796 kPa^{-1} (applied pressure $\leq 2 \text{ kPa}$). In addition, the flexible pressure sensor has a low limit of detection of 4 Pa and a fast response time of 65 ms , and its performance remains unchanged after 1000 loading/unloading tests. This high performance enables flexible pressure sensors to detect touch and limb movement. Considering the good performance of the device, we expect that the sensor will provide broad application prospects in the fields of smart electronics and artificial intelligence.

Keywords Porous PDMS · capacitive pressure sensor · wearable

Introduction

Recently, electronic skin (e-skin) has demonstrated broad development prospects in applications such as intelligent robots,^{1,2} human–computer interaction,^{3,4} human health monitoring,^{5–7} and wearable mobile devices.^{8–10} As the core of e-skin, the performance of the flexible pressure sensor (FPS) determines the overall performance of the electronic skin. In general, pressure sensors can be divided into four types according to their sensing mechanism: piezoresistive,^{11–13} capacitive,^{14,15} piezoelectric,^{16–18} and triboelectric.^{19–21} The capacitive pressure sensor has the advantages of simple structure, low manufacturing cost, and low power consumption compared with other types of sensors. Capacitive pressure sensors generally consist of two parallel electrodes and a dielectric layer. The capacitance can

be effectively tuned by changing the distance between the electrodes. In other words, the goal is to produce large spacing variations within small pressure ranges. Therefore, the dielectric layer is a key component to improve the sensitivity of the capacitive pressure sensor. Polydimethylsiloxane (PDMS) is the most widely used dielectric material for capacitive pressure sensor because it is highly deformable, eco-friendly, transparent, and biocompatible, which makes it especially suitable as artificial skin. Some studies have shown that dielectric layers with structures which are easily compressed can effectively improve the sensitivity and corresponding characteristics of FPS. Therefore, the structure of the dielectric layer becomes the key to improving the sensitivity of the sensor.

In recent years, various dielectric layer structures have been studied to improve sensor performance, such as pyramids,^{14,22,23} porous structures,^{24–27} and micro-pillar structures,²⁸ which can induce large deformation under subtle external stimuli. For example, researchers use photolithography to carve pyramid-shaped and cone-shaped templates on silicon wafers, and use PDMS inverted molds to obtain pyramid- and cone-shaped microstructure films; the tips of these patterns are easily deformed. However, although the sensitivity of the sensor made by the microstructure pattern method has been improved, the pattern will collapse rapidly under low pressure, so the measurement range is low

✉ Wenxing An
anwenxing@tju.edu.cn

✉ Shihui Yu
ysh728@126.com

¹ School of Microelectronics, Tianjin University,
Tianjin 300072, People's Republic of China

² Department of Electrical Engineering and Automation,
Luoyang Institute of Science and Technology,
Luoyang 471023, Henan, China

(0–1 kPa). In addition, the procedure for preparing silicon templates is more complicated and more costly. On the other hand, the porous structure has a large specific surface area, and large volume changes can occur under pressure, leading to high sensitivity and a wide range of detection; thus, it has been widely used in capacitive pressure sensors. At present, the porous structure is generally prepared by three methods: emulsion template, particle template, and chemical foaming methods. Porous polydimethylsiloxane (P-PDMS) has been prepared simply by evaporating the dispersed phase using the emulsion template method.^{27,29} Kang et al.³⁰ used microwaves to process the mixed solution of perfluorocarbon and PDMS to form a porous structure. These micropores are easily deformed under small external pressure, so the sensor prepared in this way can detect small forces. However, the micropores will close when subjected to a small force, so the measurement range of the sensor using the emulsion template method is relatively narrow. The particle template method is a traditional strategy which offers a simple and inexpensive means for preparing high-deformation PDMS with good reproducibility and repeatability. This method creates pores by adding solid particles such as polystyrene (PS) balls and salt or sugar crystals^{24,31} to uncured PDMS. For example, Wei et al.³² formed a porous structure by dissolving sodium chloride (NaCl) particles mixed in a PDMS–carbon conductive paste (CCP) composite material. The sensor made using this method has a wide measurement range, but the gap inside the PDMS is relatively large and requires high pressure to be completely closed, so the sensitivity of the sensor is low. In addition, it is difficult to completely remove the added particles. Another effective method for preparing porous structures is the chemical foaming process, which produces P-PDMS by creating bubbles during curing. For example, NaHCO_3 and NH_4Cl particles are added to uncured PDMS,^{33,34} and these particles are heated and decomposed to produce gas to form a porous structure. The disadvantage of this method is that it will produce some harmful gases, with adverse effects on the environment.

In this work, a simple and innovative method based on the physical foaming technique is proposed to spontaneously form a porous structure under heating. It does not require custom templates, complex processes, or expensive equipment, which opens an avenue for the low-cost and controllable commercial manufacture of microstructures economically and efficiently. Pressure sensors made using this method have a wide measurement range and high sensitivity. The sensitivity of the flexible capacitor pressure sensor is as high as 0.796 kPa^{-1} , the response time is 65 ms, the detection limit is as low as 4 Pa, and the sensor can be reused at least 1000 times. In addition, the application of FPS in human motion and intelligent robots is investigated in this work, which illustrates that the FPS fabricated in our work has broad application prospects.

Experimental Section

Raw Materials and Fabrication Process

Polyethylene terephthalate-indium tin oxide (PET-ITO) flexible conductive substrate (square resistance: 30–35 Ω/sq , light transmittance: > 86%) was purchased from Zhuhai Kaiwei Optoelectronics Technology Co., Ltd. Deionized water was made by the laboratory. *Paulownia*, pine, and beech were purchased from Shandong Caoxian Tianlong Wood Products Factory. The conductive silver paste was purchased from Carson Co., Ltd. The PDMS elastomer (Sylgard 184) was purchased from Dow Corning Co., Ltd.

The preparation of the porous-structured sensor was carried out as follows: Firstly, a PDMS mixture was prepared with basic glue and curing agent in a mass ratio of 10:1. The pine was cut into small pieces of $1 \text{ cm} \times 1 \text{ cm} \times 0.5 \text{ cm}$, and the PDMS mixture was spin-coated on the surface of the wooden block (the rotational speed of the homogenizer was 650 rpm, the time was 15 s). The PDMS with a porous structure was stripped after curing at 120°C for 1 h. Subsequently, the P-PDMS surfaces were cleaned with deionized water and dried in an oven at 80°C . Next, the P-PDMS and the PET-ITO film were both cut into pieces of $0.7 \text{ cm} \times 0.7 \text{ cm}$, and the conductive silver paste was used to fix the wire on the conductive layer of the PET-ITO film. Then the PET-ITO film of the lead wire was used as the upper and lower electrodes of the sensor, and the P-PDMS was used as the dielectric layer. Finally, the edges were bonded together using 3M Scotch tape to assemble the sandwich-structured FPS.

Characterization

The surface morphology of the PDMS patterned layer was investigated by field emission scanning electron microscopy (SEM, JEOL JSM-6700F, Japan). The capacitance was measured using an inductance capacitance and resistance (LCR) meter (TongHui TH2830). External pressure was applied using a force gauge with computer-controlled stages (Shanghai Kanyan Testing Instrument Co., LTD). A laboratory-made electromagnet/relay test system was used for cyclic loading/unloading tests.

Results and Discussion

Properties of P-PDMS Composites as Dielectric Layers

Figure 1a shows the preparation process for the porous structure sensor: The PDMS pre-solidified liquid is spin-coated

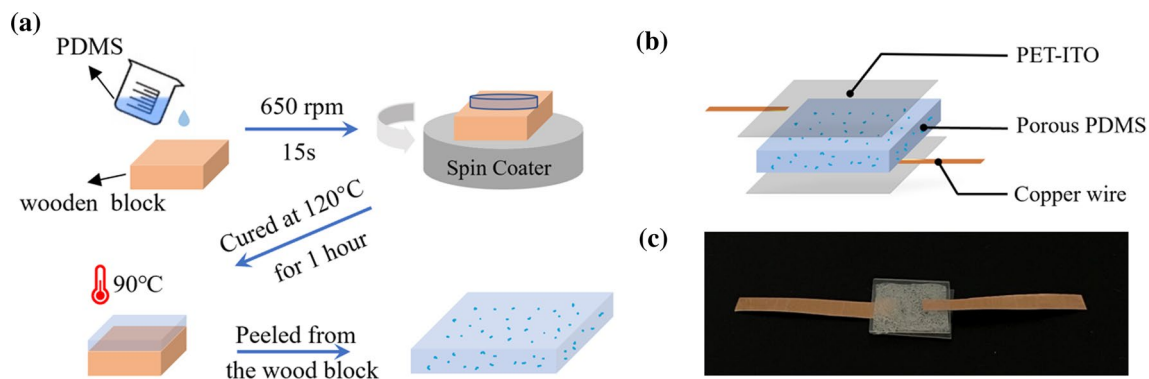


Fig. 1 Preparation of the P-PDMS and FPS. (a) Flow chart of P-PDMS structure. (b) The structure of the P-PDMS composite-based capacitive pressure sensor. (c) Photograph of the capacitive pressure sensor fabricated with the P-PDMS dielectric layer.

on the surface of the wood block, and the PDMS/wood block is heated and cured. During the curing process, the air in the gap of the wood block will be heated and will rise into the PDMS to form a porous structure. Finally, PET-ITO is used as the electrodes of the sensor. A photograph and schematic illustration of the sensors is presented in Fig. 1b and c. The prepared sensor dielectric layer becomes loose and opaque due to the existence of bubbles.

During the PDMS curing process, the air in the cracks of the wood blocks will be heated and will rise into the PDMS to form bubbles. The wood density and temperature can affect the number of bubbles in the PDMS. In order to explore the impact of different types of wood on the sensitivity of the sensor, we selected three kinds of wood for comparative experiments. The density of *Paulownia* is 2.72 g/cm³, and Young's modulus is 3740 MPa³⁵; the density of pine is 0.5 g/cm³, Young's modulus is 986 MPa, and the Poisson ratio is 0.651³⁶; the density of beech is 0.745 g/cm³, Young's modulus is 2240 MPa, and the Poisson ratio is 0.36.³⁷ The capacitance change curves of the three densities are shown in Fig. 2a. We generally use sensitivity to evaluate the performance of the sensor. The sensitivity of a capacitive pressure sensor is defined as follows:

$$S = \delta(\Delta C/C_0)/\delta P \quad (1)$$

where C_0 is the initial capacitance, ΔC is the relative change in capacitance, and P is the applied pressure.³⁸ Therefore, the greater the change in capacitance per unit of pressure, the higher the sensitivity of the sensor. According to this formula, we can evaluate the sensitivity of the sensor by calculating the slope of the $(\Delta C/C_0) - P$ curve, which can be divided into two linear regions. The variation in the capacitance of the P-PDMS capacitive pressure sensors increases logarithmically under applied pressure. When the pores close under pressure, the capacitance variation gradient is reduced.^{9,39} The porous structure sensor made of

Paulownia has sensitivity of 0.796 kPa⁻¹ when the pressure is lower than 2 kPa, and the sensitivity is 0.081 kPa⁻¹ when the pressure is higher than 2 kPa. The porous sensor made of pine wood has sensitivity of 0.532 kPa⁻¹ and 0.039 kPa⁻¹ when the pressure is lower and higher than 2 kPa, and the porous structure sensor made of beech wood has sensitivity of 0.279 kPa⁻¹ and 0.023 kPa⁻¹ when the pressure is lower than and higher than 2 kPa, respectively. *Paulownia* has the lowest density (0.3 g/cm³) among these three wood blocks, so the number of pores in *Paulownia* is the greatest under the same area. Figure 2b shows a microscopic image of the surface of the three kinds of wood blocks. It can be seen that there are many pores on the surface of *Paulownia* wood, and there are almost no pores on the surface of beech wood. The sensor with the porous structure made of *Paulownia* has the highest sensitivity because the greatest number of air bubbles is in the PDMS templated with *Paulownia*. Therefore, we chose *Paulownia* as the template for the porous structure sensor. Figure 3 shows SEM images of the surface and cross-section of the P-PDMS. There are a large number of bubbles in the PDMS, and most of the bubbles are 150 μ m in diameter. The bubbles are regular spherical and evenly distributed in the PDMS.

To explore the influence of curing temperature on the porous structure, we used *Paulownia* wood as a template to solidify PDMS at 60°C, 80°C, 100°C, 120°C, and 140°C. Figure 2d shows a microscopic image of the surface of the P-PDMS structure at different temperatures. The number of bubbles per unit area increases with increasing temperature, but no change is seen in the number of bubbles generated per unit area beyond a temperature of 100°C (Fig. 2c). As the heating causes the air to rise, the air rises faster and more bubbles enter the PDMS when the temperature is higher. At the same time, the curing speed of PDMS also accelerates with the rise in temperature, and the bubbles which enter the PDMS can remain in the PDMS. The rate of rising air is slower and fewer bubbles

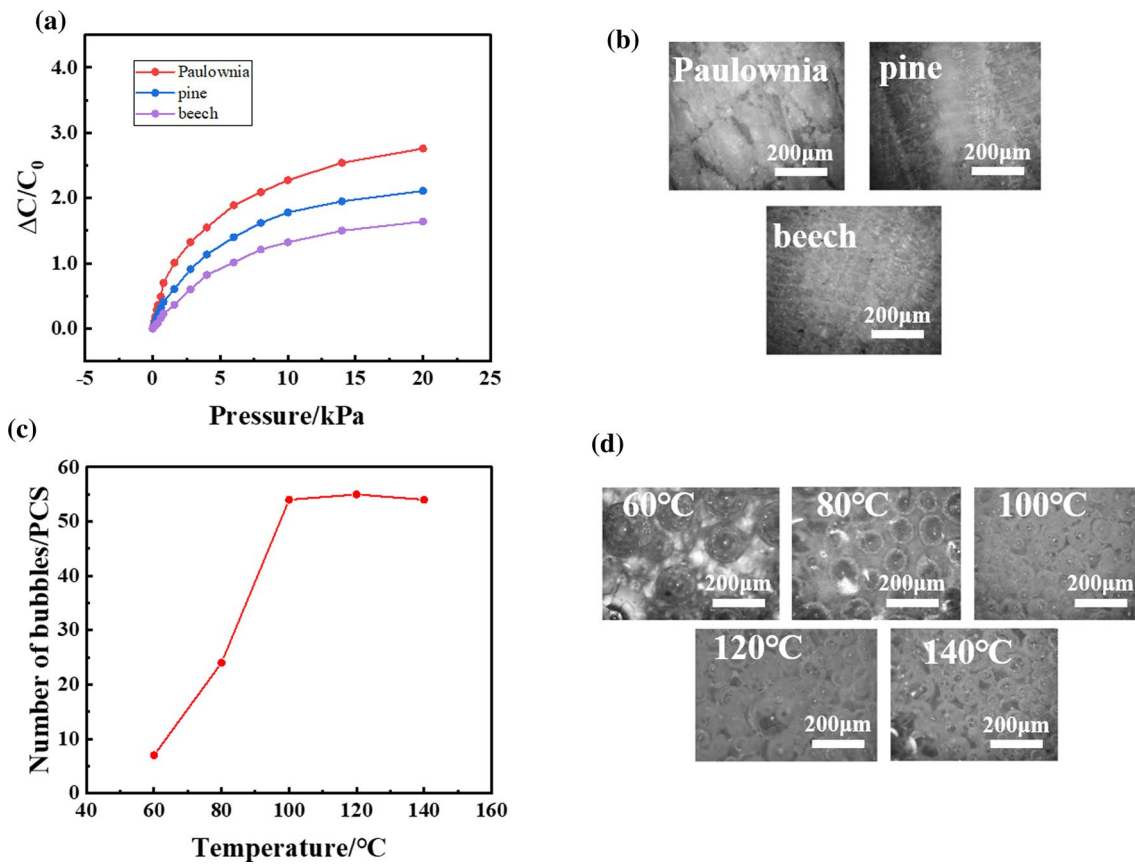


Fig. 2 Influencing factors of porous structure performance. (a) Sensitivity of sensors with different wooden blocks as templates. (b) The microscope image of the surface of different wood blocks. (c) The

number of bubbles per unit area at different temperatures. (d) The microscope images of the P-PDMS structure surface at different temperatures.

enter the PDMS when the temperature is lower. At the same time, the curing speed of PDMS is slower. The bubbles entering PDMS gradually rise into the air, and fewer bubbles remain in PDMS. When the temperature is increased to 100 $^{\circ}\text{C}$, the maximum rate of air and curing speed of PDMS are reached. With curing above 100 $^{\circ}\text{C}$, the number of bubbles in the P-PDMS remains unchanged, so we chose 100 $^{\circ}\text{C}$ as the curing temperature for PDMS. The influence of bubbles in the P-PDMS structure on the sensitivity is mainly due to the following. The definition of capacitance is:

$$C = \epsilon_0 \epsilon_r \frac{A}{d} \quad (2)$$

where ϵ_0 is the dielectric constant of air, ϵ_r is the dielectric constant of the dielectric layer, A is the overlapping area of the two electrodes, and d is the distance between the two electrodes.⁴⁰ The P-PDMS is more likely to deform than unstructured PDMS under the same pressure because it is composed of many pores (air).

The low dielectric constant of the pores ($\epsilon_0=1$) is replaced by the high dielectric constant of PDMS ($\epsilon_{PDMS}=2.7$) as the

pores close with increasing pressure.¹⁰ The effective dielectric constant of the P-PDMS composites is:

$$\epsilon_e = \epsilon_0 \frac{V_{\text{air}}}{V_{\text{air}} + V_{PDMS}} + \epsilon_{PDMS} \frac{V_{PDMS}}{V_{\text{air}} + V_{PDMS}} \quad (3)$$

where V_{air} is the volume of air in P-PDMS, and V_{PDMS} is the volume of PDMS in P-PDMS.³¹ When pressure is applied, V_{air} decreases while V_{PDMS} is almost constant, which causes $\frac{V_{PDMS}}{V_{\text{air}} + V_{PDMS}}$ to increase, thereby increasing the effective dielectric constant of P-PDMS. Therefore, the P-PDMS dielectric layer sensor with high porosity has high sensitivity.

Performance of the Sensor

In order to study the influence of the bubble structure on the performance of the sensor, unstructured PDMS with the same dielectric layer thickness was used as the dielectric layer of the sensor for comparison. Figure 4a shows the sensitivity of two types of sensors. The slope of the curve can be divided into two linear regions. The sensor with a bubble

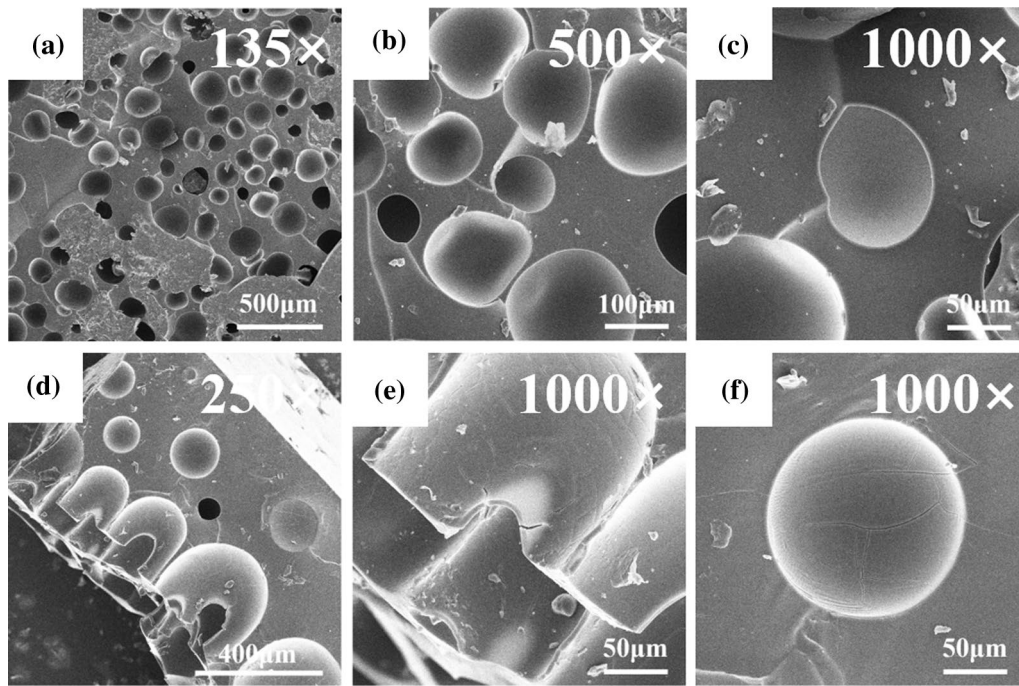


Fig. 3 SEM image of P-PDMS. (a) The front image of the porous structure. (b) A partial image of the front of the porous structure at $\times 500$ magnification. (c) A partial image of the front of the porous structure at $\times 500$ magnification. (d) The cross-sectional image of the

porous structure. (e) A partial image of a cross section of the porous structure at $\times 1000$ magnification. (f) The partial image of a cross section of the porous structure at $\times 1000$ magnification.

structure has sensitivity of 0.796 kPa^{-1} when the pressure is lower than 2 kPa and 0.081 kPa^{-1} when the pressure is higher than 2 kPa, and the unstructured sensor has sensitivity of 0.092 kPa^{-1} and 0.017 kPa^{-1} at pressures below and above 2 kPa, respectively. We can see from Fig. 4a that the porous structure improves the sensitivity significantly. There are two main reasons for this high sensitivity. The first is that P-PDMS is composed of many pores (air), so the P-PDMS is more easily deformed than unstructured PDMS under the same pressure. The second reason is that the high dielectric constant of PDMS ($\epsilon_{PDMS}=2.7$) replaces the low dielectric constant ($\epsilon_0=1$) of the pores during the process of pore closing with increasing pressure, which increases the capacitance change.

In addition, an object with a low weight (20 mg) was loaded on the sensor to explore the detection limit and the response time of the microstructure flexible pressure sensor (MFPS). As shown in Fig. 4b, the capacitance of the sensor increases rapidly within a response time of 65 ms and remains at a stable value when the pressure is loaded. The capacitance of the sensor drops rapidly and decays to the initial value within 117 ms as the pressure is unloaded (inset of Fig. 4b). This means that the sensor proposed in this work has sufficient practicality in real-life applications.⁴¹ The loading response time is faster than the recovery time, which can be attributed to the structure

deformed by external forces during the loading process and the dependence of the recovery process on the nature of the material itself. The viscoelastic behavior of the PDMS film may be another reason.^{42–44} The repeatability test instrument was made by the laboratory. We first placed the sensor on the electromagnet, then placed a thin iron sheet on the sensor, and used a timing relay to control the on and off cycles of the electromagnet, so that each on and off cycle of the electromagnet could complete a loading/unloading cycle. We carried out 1000 loading/unloading tests on the sensor. The illustration in Fig. 4c shows the signals of the three different stages of the repeated test, and the waveform is basically identical. The results show that there is no fatigue in the sensor over 1000 loading/unloading cycles due to the good elasticity of PDMS. In order to explore the stability of the sensor, the sensor was put into a constant temperature and humidity chamber at 85°C and 85% relative humidity for an aging test. As shown in Fig. 5, the sensitivity of the sensor remained unchanged after 72 h, indicating its good stability. In addition, a performance comparison between this work and sensors reported in recent years is shown in Table I. It can be seen that the sensor has good performance. From the above experimental results, we can see that our microstructural sensors have high sensitivity, a low detection limit, and good stability and reliability.

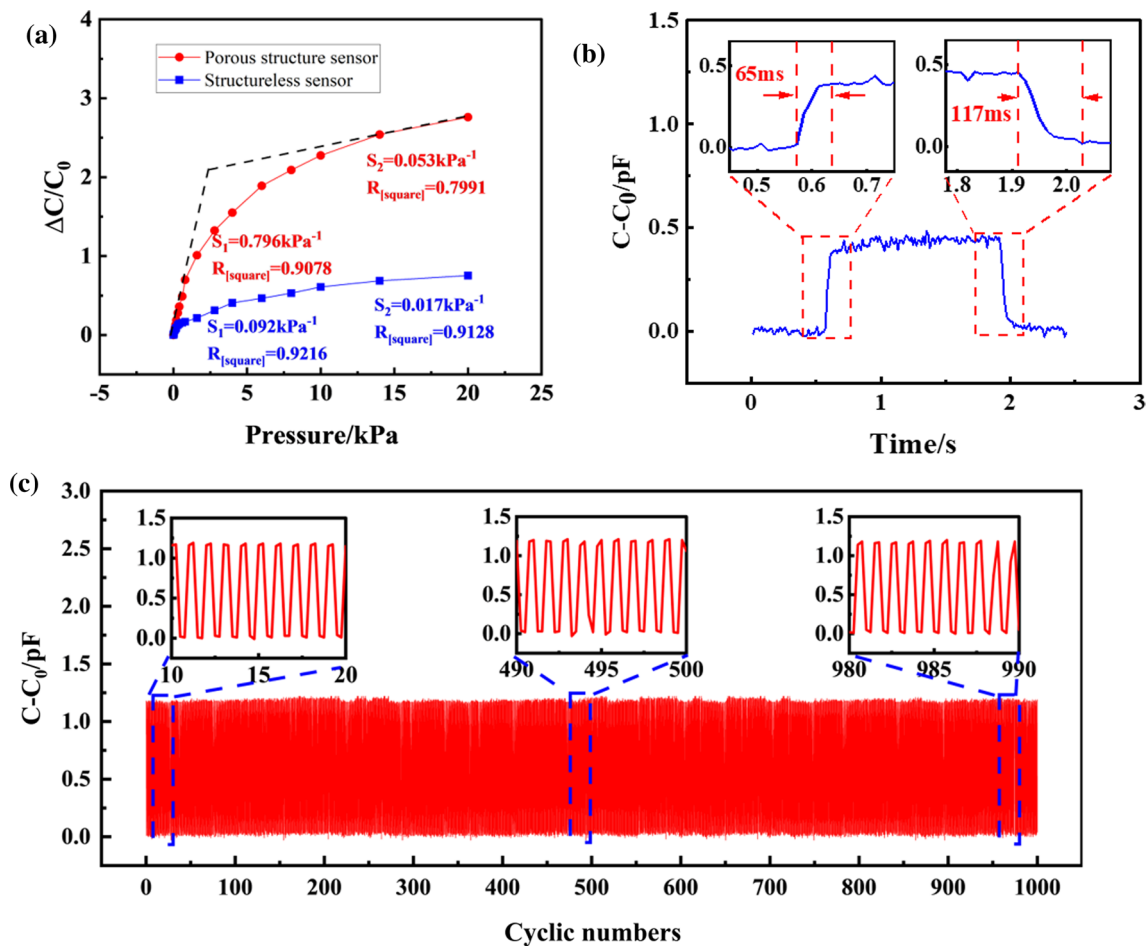


Fig. 4 Properties of the tactile sensors. (a) Sensitivity of the porous structure (red circles) and structureless sensor (blue squares). (b) Real-time response of the sensor to an ultralow pressure of 4 Pa. The insets show the response time upon loading and unloading. (c) The

reliability of the sensor was tested for 1000 cycles under applied pressure of 0.5 kPa, and the insets show signals under the different number of cycles (Color figure online).

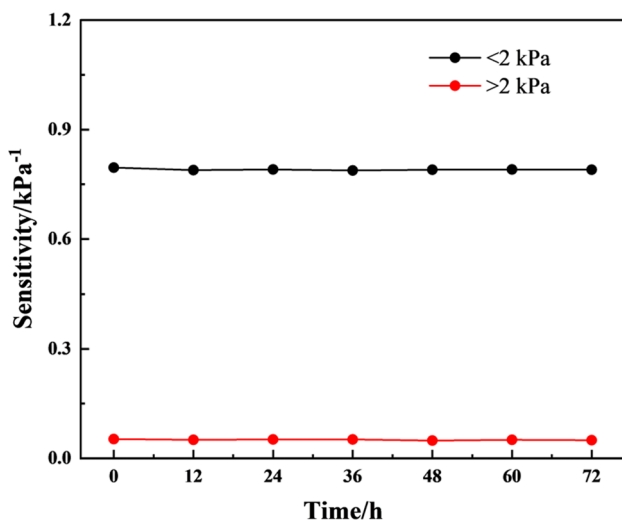


Fig. 5 The stability test of the sensor in a constant temperature and humidity chamber at 85°C and 85% relative humidity.

Application in Wearable Electronics

Based on the basic mechanism of the sensor and excellent sensing performance, Fig. 6 shows some applications in human motion detection and intelligent robots. As shown in Fig. 6a and b, the sensor is attached onto the surface of the left mouse button to monitor the human body for mouse clicks. Stable dynamic signals generated by the sensor can be seen by clicking and double-clicking the mouse, and the single-click and double-click signals can be distinguished, which provides an idea for the development of the mouse in the future. In addition, the sensor can be used in electronic skin, as the pressure sensor can provide feedback to the robot similar to “tactile” feedback, so that the robot can complete its work reliably and accurately. As shown in Fig. 6c and d, a sensor was installed on the thumb, and then the beaker was held by hand. The changes in pressure signals could be seen by adding 100 ml water

Table 1 Comparison of this work with capacitive pressure sensors in recent years

No.	Material and structure	Working range	Sensitivity	Response time [ms]	Ref.
1	Ag@Ni/CMRF	< 145 kPa	0.159 kPa ⁻¹ at 0–1 kPa, 0.019 kPa ⁻¹ at 1.5–11 kPa	50	45
2	DMESA	< 100 kPa	0.86 kPa ⁻¹ at 10 Pa	100	46
3	Au-coated PDMS Reed leaves	< 40 kPa	0.6 kPa ⁻¹ at 0–1 kPa	180/120	47
4	CNT-PVDF	< 15 kPa	0.99 kPa ⁻¹ at 0–1.2 kPa	29	48
5	Nylon netting/GrPDMS	< 5 kPa	0.33 kPa ⁻¹ at 1 kPa	20	49
This work	PDMS	< 25 kPa	0.796 kPa ⁻¹ at 0–2 kPa, 0.053 kPa ⁻¹ at 2–25 kPa	65	

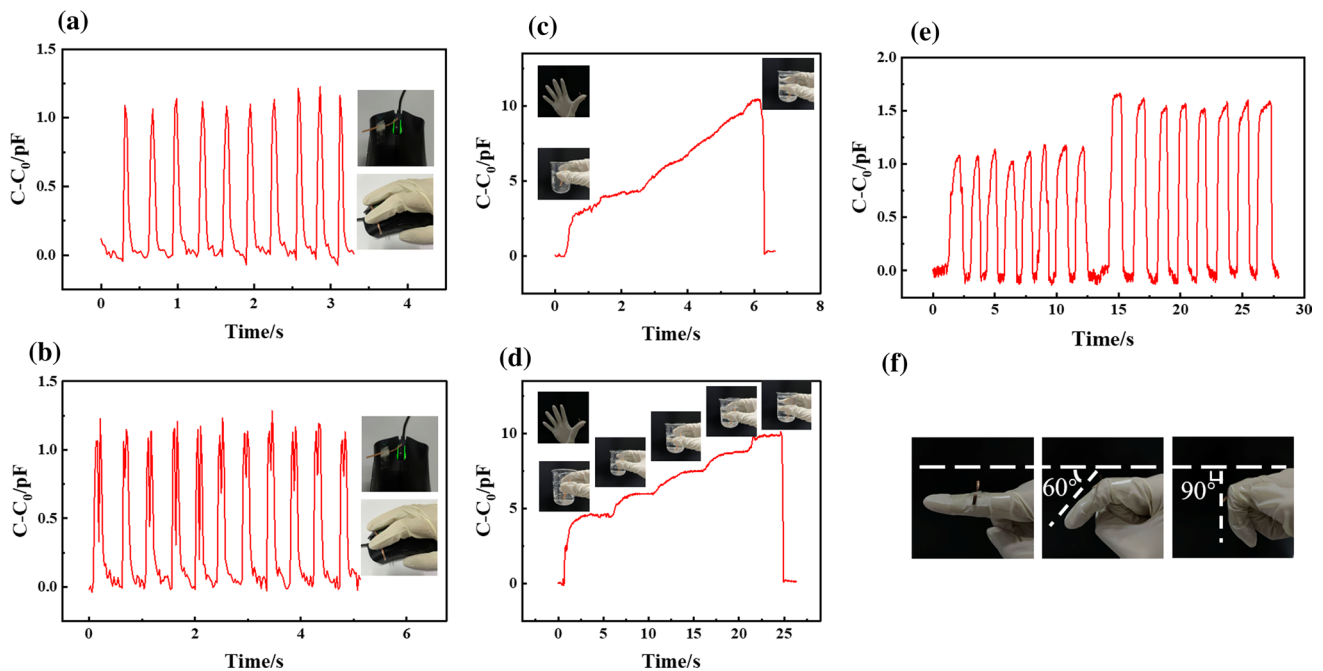


Fig. 6 Application of porous structure sensor. (a) The number of capacitance changes when the mouse is clicked. (b) The number of capacitance changes when the mouse is double-clicked. (c) Adding

water at a constant rate in the beaker. (d) Adding water several times in the beaker. (e) The number of capacitance changes for different bending angles of the finger. (f) Different bending angles of fingers.

at a constant rate and 20 ml water several times in the beaker. The pressure sensor could easily measure the force of the thumb, which shows that the sensor can play an important role in the tactile perception of the manipulator. Furthermore, the flexible sensor can also be used for daily monitoring of the human body. Figure 6f shows that the pressure sensor is installed at the index finger joint. A significant change in capacitance can be seen (Fig. 6e) with the different bending angles of the knuckle. The force on the sensor increases with the increase in the bending angle, so as the bending angle increases, the sensor generates stronger signals, increasing the variation. The bending radius can be calculated by the following expression:

$$\begin{cases} \frac{d}{2r} = \sin\left(\frac{L}{2r}\right) & (d > \frac{2l}{\pi}) \\ r = \frac{d}{2} & (d < \frac{2l}{\pi}) \end{cases} \quad (4)$$

where L defines the length of the sensor and d defines the distance between the ends of the sensor. From the above formula, it can be calculated that the bending radius is 3.7 mm when the bending angle is 120°, and the bending radius is 2.45 mm when the bending angle is 90°. This suggests that the flexible tactile sensor can be used as a skin-mountable wearable sensor to monitor human motion.

Conclusion

In conclusion, we propose a low-cost and simple method for preparing porous structures. The capacitive sensor uses P-PDMS as the dielectric layer and PET-ITO as the upper and lower electrodes. The sensitivity of the FPS is 0.796 kPa^{-1} (applied pressure $< 2 \text{ kPa}$), which is significantly higher than that of an unstructured sensor. In addition, the FPS has a low detection limit of 4 Pa and fast response time within 65 ms , and its performance remains unchanged after 1000 loading/unloading tests. This high performance enables FPS to detect touch and limb movement. Considering the good performance of the device, we expect that the sensor will provide broad application prospects in the fields of smart electronics and artificial intelligence.

Author Contributions All authors contributed to the study conception and design. Material preparation, data collection and analysis were performed by ZS, LZ, CC, YZ, SY and WA. The first draft of the manuscript was written by ZS, and all authors commented on previous versions of the manuscript. All authors read and approved the final manuscript.

Funding This work is supported by the National Natural Science Foundation of China (Grant No. 52175525) and Science and Technology Project of Henan Province (No. 202102210277).

Data Availability The authors declare that all data supporting the findings of this study are available within the article.

Conflict of interest On behalf of all authors, the corresponding author states that there is no conflict of interest.

References

- W. Asghar, F.L. Li, Y.L. Zhou, Y.Z. Wu, Z. Yu, S.B. Li, D.X. Tang, X.T. Han, J. Shang, Y.W. Liu, and R.W. Li, Piezocapacitive Flexible E-Skin Pressure Sensors Having Magnetically Grown Microstructures. *Adv. Mater. Technol.* 5, 9 (2020).
- Y. Zhang, C. Lingfei, and R. Zhang, PEG-assisted Hydrothermal Synthesis of Porous $\text{Li}_3\text{V}_2(\text{PO}_4)_3$ Frameworks for Lithium-ion Batteries. *Emergent Mater.* 3, 331–337 (2020).
- R.Y. Tay, H. Li, J. Lin, H. Wang, J.S.K. Lim, S. Chen, W.L. Leong, S.H. Tsang, and E.H.T. Teo, Lightweight, Superelastic Boron Nitride/Polydimethylsiloxane Foam as Air Dielectric Substitute for Multifunctional Capacitive Sensor Applications. *Adv. Funct. Mater.* 30, 1909604 (2020).
- S. Yu, X. Liu, P. Yang, L. Zhao, H. Dong, C. Wu, X. Li, and J. Xiong, Highly Stable Silver Nanowire Networks with tin Oxide Shells for Freestanding Transparent Conductive Nanomembranes Through All-Solution Processes. *Chem. Eng. J.* 446, 137481 (2022).
- Y. Gao, L. Yu, J.C. Yeo, and C.T. Lim, Flexible Hybrid Sensors for Health Monitoring: Materials and Mechanisms to Render Wearability. *Adv. Mater.* 32, 1902133 (2020).
- X. Wang, O. Yue, X. Liu, M. Hou, and M. Zheng, A Novel Bio-Inspired Multi-Functional Collagen Aggregate Based Flexible Sensor with Multi-Layer and Internal 3D Network Structure. *Chem. Eng. J.* 392, 123672 (2020).
- S. Yu, X. Liu, P. Yang, C. Wu, and L. Li, Flexible Transparent Ag Nanowire/UV-Curable Resin Heaters with Ultra-Flexibility, high Transparency, Quick Thermal Response, and Mechanical Reliability. *J. Alloys. Comps* 908, 164690 (2022).
- O. Atalay, A. Atalay, J. Gafford, and C. Walsh, A Highly Sensitive Capacitive-Based Soft Pressure Sensor Based on a Conductive Fabric and a Microporous Dielectric Layer. *Adv. Mater. Technol.* 3, 1700237 (2018).
- Z. Song, Y. Zhou, L. Zhao, C. Chang, W. An, and S. Yu, A Wearable Capacitive Friction Force Sensor for E-Skin. *ACS Appl. Electron. Mater.* (2022). <https://doi.org/10.1021/acsaelm.2c00463>.
- J. Lee, H. Kwon, J. Seo, S. Shin, J.H. Koo, C. Pang, S. Son, J.H. Kim, Y.H. Jang, D.E. Kim, and T. Lee, Conductive Fiber-Based Ultrasensitive Textile Pressure Sensor for Wearable Electronics. *Adv. Mater.* 27, 2433–2439 (2015).
- J. Lee, J. Kim, Y. Shin, and I. Jung, Ultra-Robust Wide-Range Pressure Sensor with Fast Response Based on Polyurethane foam Doubly Coated with Conformal Silicone Rubber and CNT/TPU Nanocomposites Islands. *Compos. B. Eng.* 177, 107364 (2019).
- H. Liu, H. Gao, and G. Hu, Highly Sensitive Natural Rubber/Pristine Graphene Strain Sensor Prepared by a Simple Method. *Compos. B. Eng.* 171, 138–145 (2019).
- C. Feng, Z. Yi, X. Jin, S.M. Seraji, Y. Dong, L. Kong, and N. Salim, Solvent Crystallization-Induced Porous Polyurethane/Graphene composite Foams for Pressure Sensing. *Compos. B. Eng.* 194, 108065 (2020).
- Y. Luo, J. Shao, S. Chen, X. Chen, H. Tian, X. Li, L. Wang, D. Wang, and B. Lu, Flexible Capacitive Pressure Sensor Enhanced by Tilted Micropillar Arrays. *ACS Appl. Mater. Interfaces* 11, 17796–17803 (2019).
- D. Du, X. Ma, W. An, and S. Yu, Flexible Piezoresistive Pressure Sensor Based on Wrinkled Layers with Fast Response for Wearable Applications. *Measurement* 201, 111645 (2022).
- C. Dagdeviren, P. Joe, O.L. Tuzman, K.-I. Park, K.J. Lee, Y. Shi, Y. Huang, and J.A. Rogers, Recent Progress in Flexible and Stretchable Piezoelectric Devices for Mechanical Energy Harvesting, Sensing and Actuation. *Extreme Mech. Lett.* 9, 269–281 (2016).
- W. Wang, Y. Zheng, X. Jin, Y. Sun, B. Lu, H. Wang, J. Fang, H. Shao, and T. Lin, Unexpectedly High Piezoelectricity of Electrospun Polyacrylonitrile Nanofiber Membranes. *Nano Energy* 56, 588–594 (2019).
- S. Luo, X. Zhou, X. Tang, J. Li, D. Wei, G. Tai, Z. Chen, T. Liao, J. Fu, D. Wei, and J. Yang, Microconformal Electrode-Dielectric Integration for Flexible Ultrasensitive Robotic Tactile Sensing. *Nano Energy* 80, 105580 (2021).
- K.Y. Lee, H.-J. Yoon, T. Jiang, X. Wen, W. Seung, S.-W. Kim, and Z.L. Wang, Fully Packaged Self-Powered Triboelectric Pressure Sensor Using Hemispheres-Array. *Adv. Energy Mater.* 6, 1502566 (2016).
- V.K.S. Hsiao, S.-F. Leung, Y.-C. Hsiao, P.-K. Kung, Y.-C. Lai, Z.-H. Lin, K.N. Salama, H.N. Alshareef, Z.L. Wang, and J.-H. He, Photo-Carrier Extraction by Triboelectricity for Carrier Transport Layer-Free Photodetectors. *Nano Energy* 65, 103958 (2019).
- T.Y. Zhong, M.Y. Zhang, Y.M. Fu, Y.C. Han, H.Y. Guan, H.X. He, T.M. Zhao, L.L. Xing, X.Y. Xue, Y. Zhang, and Y. Zhan, An Artificial Triboelectricity-Brain-Behavior Closed Loop for Intelligent Olfactory Substitution. *Nano Energy* 63, 9 (2019).
- Y. Xiong, Y. Shen, L. Tian, Y. Hu, P. Zhu, R. Sun, and C.-P. Wong, A Flexible, Ultra-Highly Sensitive and Stable Capacitive Pressure Sensor with Convex Microarrays for Motion and Health Monitoring. *Nano Energy* 70, 104436 (2020).
- J. Pignatelli, K. Schlingman, T.B. Carmichael, S. Rondeau-Gagne, and M.J. Ahamed, A Comparative Analysis of Capacitive-Based Flexible PDMS Pressure Sensors. *Sens. Actuator A Phys.* 285, 427–436 (2019).

24. J. Il Yoon, K.S. Choi, and S.P. Chang, A Novel Means of Fabricating Microporous Structures for the Dielectric Layers of Capacitive Pressure Sensor. *Microelectron. Eng.* 179, 60–66 (2017).
25. J. Hwang, Y. Kim, H. Yang, and J.H. Oh, Fabrication of Hierarchically Porous Structured PDMS Composites and their Application as a Flexible Capacitive Pressure Sensor. *Compos. B. Eng.* 211, 9 (2021).
26. W. Li, X. Jin, X. Han, Y. Li, W. Wang, T. Lin, and Z. Zhu, Synergy of Porous Structure and Microstructure in Piezoresistive Material for High-Performance and Flexible Pressure Sensors. *ACS Appl. Mater. Interfaces* 13, 19211–19220 (2021).
27. B.Y. Lee, J. Kim, H. Kim, C. Kim, and S.D. Lee, Low-Cost Flexible Pressure Sensor Based on Dielectric Elastomer Film with Micro-Pores. *Sens. Actuator A Phys.* 240, 103–109 (2016).
28. X. Chen, J. Shao, H. Tian, X. Li, C. Wang, Y. Luo, and S. Li, Scalable Imprinting of Flexible Multiplexed Sensor Arrays with Distributed Piezoelectricity-Enhanced Micropillars for Dynamic Tactile Sensing. *Adv. Mater. Technol.* 5, 2000046 (2020).
29. S. Jang, and J.H. Oh, Rapid Fabrication of Microporous BaTiO₃/PDMS Nanocomposites for Triboelectric Nanogenerators through One-step Microwave Irradiation. *Sci. Rep.* 8, 1–9 (2018).
30. Y. Kim, S. Jang, and J.H. Oh, Fabrication of Highly Sensitive Capacitive Pressure Sensors with Porous PDMS Dielectric Layer via Microwave Treatment. *Microelectron. Eng.* 215, 7 (2019).
31. S.B. Kang, J. Lee, S. Lee, S. Kim, J.K. Kim, H. Algadi, S. Al-Sayari, D.E. Kim, D. Kim, and T. Lee, Highly Sensitive Pressure Sensor Based on Bioinspired Porous Structure for Real-Time Tactile Sensing. *Adv. Electron. Mater.* 2, 8 (2016).
32. P. Wei, X. Guo, X. Qiu, and D. Yul, Flexible Capacitive Pressure Sensor with Sensitivity and Linear Measuring Range Enhanced Based on Porous Composite of Carbon Conductive Paste and Polydimethylsiloxane. *Nanotechnology* 30, 455501 (2019).
33. Y. Long, X. Zhao, X. Jiang, L. Zhang, H. Zhang, Y. Liu, and H. Zhu, A Porous Graphene/Polydimethylsiloxane Composite by Chemical Foaming for Simultaneous Tensile and Compressive Strain Sensing. *Flatchem* 10, 1–7 (2018).
34. Y. Wen, X. Liu, X. Wen, X. Chen, K. Szymanska, R. Dobrzynska, and E. Mijowska, Na₃PO₄ Assistant Dispersion of Nano-CaCO₃ Template to Enhance Electrochemical Interface: N/O/P Co-Doped Porous Carbon Hybrids Towards High-Performance Flexible Supercapacitors. *Compos. B. Eng.* 199, 108256 (2020).
35. M.H. Akyildiz, and H.S. Kol, Some Technological Properties and uses of Paulownia (PAULOWNIA Tomentosa Steud.) Wood. *J. Environ. Biol.* 31, 351–355 (2010).
36. N. Yang, and L. Zhang, Investigation of Elastic Constants and Ultimate Strengths of Korean Pine from Compression and Tension Tests. *J. Wood Sci.* 64, 85–96 (2018).
37. S. Hering, D. Keunecke, and P. Niemz, Moisture-Dependent Orthotropic Elasticity of Beech Wood. *Wood Sci. Technol.* 46, 927–938 (2012).
38. M.L. Hammock, A. Chortos, B.C. Tee, J.B. Tok, and Z. Bao, 25th Anniversary Article: The Evolution of Electronic Skin (e-skin): a Brief History, Design Considerations, and Recent Progress. *Adv Mater* 25, 5997–6038 (2013).
39. S. Yao, and Y. Zhu, Wearable Multifunctional Sensors using Printed Stretchable Conductors Made of Silver Nanowires. *Nanoscale* 6, 2345–2352 (2014).
40. Y. Wan, Y. Wang, and C.F. Guo, Recent Progresses on Flexible Tactile Sensors. *Mater. Today Phys.* 1, 61–73 (2017).
41. Y. Kim, S. Jang, B.J. Kang, and J.H. Oh, Fabrication of Highly Sensitive Capacitive Pressure Sensors with Electrospun Polymer Nanofibers. *Appl. Phys. Lett.* 111, 073502 (2017).
42. W.S. Lee, K.S. Yeo, A. Andriyana, Y.G. Shee, and F.R.M. Adikan, Effect of Cyclic Compression and Curing Agent Concentration on the Stabilization of Mechanical Properties of PDMS Elastomer. *Mater. Des.* 96, 470–475 (2016).
43. A.S. Mijailovic, B. Qing, D. Fortunato, and K.J. Van Vliet, Characterizing Viscoelastic Mechanical Properties of Highly Compliant Polymers and Biological Tissues Using Impact Indentation. *Acta Biomater.* 71, 388–397 (2018).
44. A. Dalla Monta, F. Razan, J.-B. Le Cam, G. Chagnon, Using thickness-shear mode quartz resonator for characterizing the viscoelastic properties of PDMS during cross-linking, from the liquid to the solid state and at different temperatures. *Sens. Actuator A Phys.* 280, 107–113 (2018).
45. W. Asghar, F. Li, Y. Zhou, Y. Wu, Z. Yu, S. Li, D. Tang, X. Han, J. Shang, and Y.J.A.M.T. Liu, Piezocapacitive Flexible E-Skin Pressure Sensors Having Magnetically Grown Microstructures. *Adv. Mater. Technol* 5, 1900934 (2020).
46. J.O. Kim, S.Y. Kwon, Y. Kim, H.B. Choi, J.C. Yang, J. Oh, H.S. Lee, J.Y. Sim, and S. Park, Interfaces, Highly Ordered 3D Microstructure-Based electronic skin Capable of Differentiating Pressure, Temperature, and Proximity. *ACS Appl. Mater.* 11, 1503–1511 (2018).
47. Y.-Q. Liu, J.-R. Zhang, D.-D. Han, Y.-L. Zhang, and H.-B.J.A. Sun, Interfaces, Versatile Electronic Skins with Biomimetic Micronanostructures Fabricated Using Natural Reed Leaves as Templates. *ACS Appl. Mater.* 11, 38084–38091 (2019).
48. X. Yang, Y. Wang, X.J.S. Qing, and A.A. Physical, A Flexible Capacitive Sensor Based on the Electrospun PVDF Nanofiber Membrane with Carbon Nanotubes. *Sens. Actuator A Phys.* 299, 111579 (2019).
49. Z. He, W. Chen, B. Liang, C. Liu, L. Yang, D. Lu, Z. Mo, H. Zhu, Z. Tang, and X. Gui, Interfaces, Capacitive Pressure Sensor with High Sensitivity and Fast Response to Dynamic Interaction Based on Graphene and Porous Nylon Networks. *ACS Appl. Mater.* 10, 12816–12823 (2018).

Publisher's Note Springer Nature remains neutral with regard to jurisdictional claims in published maps and institutional affiliations.